Control of glucose phosphorylation in L6 myotubes by compartmentalization, hexokinase, and glucose transport

Richard R. WHITESELL*[1], Hossein ARDEHALI*[2], Richard L. PRINTZ*, Joseph M. BEECHEM*[3], Susan M. KNOBEL*, David W. PISTON*, Daryl K. GRANNER*†‡, Wieb VAN DER MEER§, Laureta M. PERRIOTT† and James M. MAY*†‡

*Department of Molecular Physiology and Biophysics, Vanderbilt University School of Medicine, Nashville, TN 37232-6303, U.S.A., †Veteran Affairs Medical Center, Nashville, TN 37232, U.S.A., ‡Department of Medicine, Vanderbilt University School of Medicine, Nashville, TN 37232-6303, U.S.A., and §Department of Physics, Western Kentucky University, Bowling Green, KY 38602, U.S.A.

In muscle, insulin enhances influx of glucose and its conversion to glucose 6-phosphate (G6P) by hexokinase (HK). While effects of insulin on glucose transport have been demonstrated, its effect on the activity of HK of cells has not. In L6 myotubes treated for 24 h with insulin there was increased expression of the HK isoform, HKII, and increased glucose phosphorylation without a concomitant increase in glucose transport, indirectly suggesting that phosphorylation of glucose was a target of insulin action [Osawa, Printz, Whitesell and Granner (1995) Diabetes **44**, 1426–1432]. In the present work the same treatment led to a 2-fold rise in G6P, suggesting that transport and/or HK were important targets of insulin action. We used a method to identify the site of rate control involving the specificity of phosphorylation towards 2-deoxy-[1-^{14}C]glucose and D-[2-^{3}H]glucose. Glucose transport does not greatly discriminate between these two tracers while HK shows increased specificity for glucose. Specificity of the glucose phosphorylation of the cells increased with addition of insulin and when extracellular glucose was raised. Specificity was reduced at low glucose concentrations or when the inhibitor of transport, cytochalasin B, was added. We conclude that transport and HK share nearly equal control over glucose phosphorylation in these cells. A computer program was used to test models for compatibility with the different types of experiments. The predicted intracellular glucose and transport rates associated with phosphorylation activity were lower than their measured values for the whole cell. In the most likely model, $15 \pm 4\,\%$ of the glucose transporters serve a proportionate volume of the cytoplasm. Insulin activation of glucose phosphorylation might then result from stimulation of these transporters together with HK recruitment or relief from inhibition by G6P.

Key words: flux control coefficient, global analysis, hexose specificity, hexose transport, sensitivity analysis.

INTRODUCTION

Glucose phosphorylation in skeletal muscle is determined primarily by glucose transport and hexokinase (HK) [1]. It is difficult to assess which step of the two is rate-determining [2], because phosphorylation of glucose has not been measured independently of its transport into cells. Actually, transport and phosphorylation were measured independently by us by following transiently the efflux and phosphorylation of glucose in frog oocytes and cultured cells after preincubation with D-[2-^{3}H]-glucose [3]. Another strategy is based on assessing substrate specificity. Glucose and 2-deoxy-glucose are transported equally well, while HK prefers glucose as its substrate [4]. Assuming the cellular milieu does not affect it, this preference can reveal the extent to which HK is rate-determining in intact myotubes [5]. A third approach tests whether transport can be rate-determining to the coupled reaction by using the transport inhibitor cytochalasin B [6]. Finally, analysis of the intracellular glucose concentration can indicate whether glucose delivery to the cytosol by the transporters matches or exceeds the ability of the HK to phosphorylate glucose. An analysis using a combination of these approaches promised to contribute to a greater understanding of the complex regulation of glucose phosphorylation by insulin in muscle.

We tested these approaches together using a line of L6 myotubes that had previously shown increased expression of HKII without a concomitant increase in glucose transport activity [7]. Since these cells show apparently little control by transport over glucose phosphorylation, they appeared to be a good model for testing the effect of insulin on phosphorylation of glucose. Modelling and analysis were combined in a program termed Global Analysis, which allows fitting of multidimensional data sets linked by common parameters [8]. Our results were incompatible with a model with one compartment for glucose phosphorylation. The data were best fit with a two-compartment model, in which active HK resides in a compartment separate from the bulk cytoplasm, and served by insulin-sensitive glucose transporters. The effect of insulin on glucose phosphorylation in this model results from co-ordinated stimulation of both transporters and HK. Although other factors such as blood supply and fibre structure contribute to the complexity of glucose uptake in intact skeletal muscle, the existence of an intracellular compartment for glucose phosphorylation can help to explain several anomalous features of the coupling of glucose transport and phosphorylation [9].

EXPERIMENTAL

Materials

All radionucleotides were from Dupont NEN (Boston, MA, U.S.A.). Cell culture media were prepared by the Vanderbilt

Abbreviations used: DMEM, Dulbecco's modified Eagle's medium; FCC, flux-control coefficient; G6P, glucose 6-phosphate; HBS, Hepes-balanced salt solution; HK, hexokinase; QAE, quaternary aminoethyl cellulose.

[1] To whom correspondence should be addressed (e-mail richard.whitesell@vanderbilt.edu).
[2] Present address: Division of Cardiology, Dept of Medicine, Johns Hopkins Hospital, 600 N Wolfe Street, Baltimore, MD 21205, U.S.A.
[3] Present address: Molecular Probes, Biosciences, Eugene, OR 97402, U.S.A.

Diabetes Research and Training Center Tissue Culture Core Facility (Nashville, TN, U.S.A.). Analytical reagents were from Sigma (St. Louis, MO, U.S.A.).

L6 myotube culture and preparation

L6 myotubes were provided by Robert J. Smith (Joslin Diabetes Center, Boston, MA, U.S.A.). Myoblasts were grown to near confluence in 24-well plates in Dulbecco's modified Eagle's medium (DMEM) containing 10 % fetal bovine serum. Myoblasts were induced to differentiate into myotubes in medium containing 2 nM tri-iodothyronine and 20 nM insulin as described previously [7]. After myotube differentiation, the medium was changed to serum-free DMEM for 48 h before an experiment. Where noted, insulin was added to a final concentration of 10 nM for the last 24 h prior to the start of measurements.

Initial uptake rates of hexoses

Immediately before the start of measurements, 1 cm-diameter wells containing approx. 5×10^5 L6 myotubes were rinsed three times with 250 μl of Hepes-balanced salt solution (HBS). This consisted of 0.2 mM glucose, 10 mM Hepes, 128 mM NaCl, 5.2 mM KCl, 1.4 mM $CaCl_2$, 1 mM Na_2HPO_4 and 1.4 mM $MgSO_4$, pH 7.5. If present before rinsing, insulin was added back in the last rinse. Other agents, such as cytochalasin B and unlabelled D-glucose or 3-*O*-methylglucose, were also included in the last rinse. After 30 min, the assay was started by substituting the medium with HBS that contained tracer amounts of two of the following: D-[2-^{3}H]glucose (0.05 μCi), L-[^{3}H]glucose (0.05 μCi), 2-deoxy-[1-^{14}C]glucose (0.0025 μCi) or 3-*O*-[^{14}C]-methylglucose (0.01 μCi). In this work, 'tracer' refers to a concentration of hexose that is much less (< 1 %) than the K_m values of the respective reactions of transport or phosphorylation in L6 myotubes.

To measure the intracellular contents of free and phosphorylated hexoses at the end of the time indicated in an experiment, the myotubes were rinsed five times in about 15 s with ice-cold HBS. It was established that these steps removed 99.9 % of extracellular sugars and ^3H_2O. The cells were extracted with 600 μl of isopropanol. A 200 μl aliquot of this extract was applied to a column containing 0.2 ml of quaternary aminoethyl cellulose (QAE–Sephadex; Amersham Biosciences) that had been converted into the chloride form. Free hexoses were eluted with 1.4 ml of water and the phosphorylated hexoses were eluted by addition of 1.4 ml of 1 M HCl directly into a 7 ml scintillation vial. Scintillation fluid was added to the samples and radioactivity was measured in a Packard CA2000 liquid scintillation spectrophotometer with windows set for dual-label counting. In other samples, the 3-*O*-[^{14}C]methylglucose space was maximal within 30 min and was taken to represent the total water space after washing. Residual extracellular space was determined from the L-[^{3}H]glucose space. The concentration of intracellular glucose was calculated as (D-[2-^{3}H]glucose space − L-[^{3}H]glucose space)/(3-*O*-[^{14}C]methylglucose space − L-[^{3}H]glucose space) × (extracellular [glucose]).

Glucose transport and phosphorylation assayed in series

The sequential coupling of transport and HK was measured as both the accumulation of phosphorylated 2-deoxy-[1-^{14}C]glucose and the release of tritium from D-[2-^{3}H]glucose. With regard to the latter, D-[2-^{3}H]glucose is transported into cells, phosphorylated by HK and the resulting glucose 6-phosphate (G6P) is converted into fructose 6-phosphate by phosphoglucose isomerase. Cycling between G6P and fructose 6-phosphate releases ^3H_2O during the isomerization step [10]. The term 'phosphorylation' for utilization of D-[2-^{3}H]glucose in intact cells is used, since the measured ^3H_2O is the product of an equilibrium reaction immediately after the phosphorylation step. In a typical experiment cells were incubated at 37 °C in HBS plus either 0.2 or 5 mM glucose and insulin as indicated. After a 30 min incubation at 37 °C, 200 μl of the medium was removed and mixed with 400 μl of isopropanol. At least 98 % of the tritium from phosphorylated D-[2-^{3}H]glucose was released as ^3H_2O, with the remainder being found in ionic glucose metabolites or in glycogen (results not shown). To measure extracellular ^3H_2O, a 60 μl sample of the fixed medium was added to a 0.2 ml column (Dowex 1 × 8 in the borate form) and eluted with 1.4 ml of water and radioactivity was counted as above.

Efflux and phosphorylation of intracellular glucose assayed in parallel

Efflux of glucose and 3-*O*-methylglucose was measured as described previously in this and other cell types [3]. Following preincubation, myotubes were incubated for 10–30 min at 37 °C with 250 μl of HBS. To this was added 10 mM glucose, 0.5 μCi of D-[2-^{3}H]glucose and 0.2 μCi of 3-*O*-[^{14}C]methylglucose (40 μM). To remove the loading medium, the HBS bathing the myotubes was rapidly replaced four times during 15 s with 250 μl of glucose-free HBS. Efflux was followed during five subsequent removals and replacements of the cell medium at 30 s intervals. At each time point, the 250 μl that was removed was fixed in 500 μl of isopropanol. These samples were assayed for unreacted D-[2-^{3}H]glucose, 3-*O*-[^{14}C]methylglucose and ^3H_2O released during the time course [3]. Following removal of the last medium sample, the remaining hexoses in the myotubes were extracted with 70 % isopropanol and assayed by anion-exchange chromatography as described above.

G6P measurements

Intracellular G6P concentrations were measured as follows. After incubation as noted in Figure 6 (see below), the myotube layer was extracted with isopropanol. Aliquots of 100 μl were applied to DEAE-cellulose filters (prepared by applying 100 μl of a 2 % slurry by weight to each well of a 96-well Packard Unifilter filter plate) and washed. Tape was applied to seal the bottom of the plate, and 30 μl of assay buffer was added. The assay buffer consisted of 30 mM KCl, 15 mM Tris, 6 mM $MgCl_2$, 1 mM $NADP^+$ and 0.2 unit/ml glucose-6-phosphate dehydrogenase (Type VII; Sigma), pH 7.5. After 20 min, fluorescence of NADPH was measured with excitation and emissions wavelength filters of 340 and 460 nm, respectively, in a plate reader (PolarStar; BMG Lab Technologies). The fluorescence of standards was significant and linear between 0.05 and 1 nmol of G6P added for a standard curve (not shown).

Measurement of HK activity

Homogenates were prepared by placing a 48-well plate of myotubes on ice and rinsing each well three times in ice-cold HBS. Homogenization buffer (50 mM triethanolamine, 100 mM KCl, 1 mM dithiothreitol, 5 % (v/v) glycerol, 1 mM EGTA, 1 mM EDTA, 1 mM PMSF, 1 μg/ml pepstatin A, 1 μg/ml leupeptin, 0.2 % sodium azide and 0.5 % Triton X-100, pH 7.5) was added and the myotubes were disrupted by three freeze–thaw cycles using dry ice and were scraped from the plate. The resulting lysate (approx. 100 μg of protein/well) was stored at −70 °C until assay of HK activity. Measurement of HK activity was based on recovery of radiolabelled sugar phosphates [11] as

modified in [12]. The assay was initiated by adding 10 μl of lysate to 90 μl of assay buffer (50 mM Tris, 20 mM $MgCl_2$, 100 mM KCl, 10 mM ATP and 1 mM dithiothreitol, pH 7.5). The latter contained the indicated concentration of unlabelled glucose, as well as 0.05 μCi of D-[U-^{14}C]glucose and 0.1 μCi of 2-deoxy-[^{3}H]glucose. After a 20 min incubation at room temperature, the reaction was stopped with the addition of 200 μl of isopropanol. A 50 μl aliquot of this solution was applied to a 0.2 ml column of QAE–Sephadex in the chloride form. The column was rinsed extensively with water, then anionic material was eluted with 1.5 ml of 1 M HCl and counted for radioactivity as above. Glucose phosphorylation by homogenates of L6 myotubes proceeded linearly for more than 90 min (results not shown). Less than 10 % of the available substrate was utilized under all conditions and the concentration of G6P contributed by the assay at termination was less than 0.05 mM at the highest glucose concentration used (5 mM). No correction for the G6P that was produced in the assay was made since the observed K_i for G6P at 10 mM ATP was greater than 0.2 mM (results not shown).

Protein was measured by the Bio-Rad assay kit (Bradford method) using BSA as a standard reference.

Imaging of cellular NAD(P)H

Two-photon laser excitation microscopy was performed using a technique described previously [13]. L6 myotubes were grown and differentiated on a coverslip-floored 35 mM dish (MatTek Corporation, Ashland, MA, U.S.A.) and incubated overnight with insulin as described above. Glucose-free HBS + 0.1 % BSA was exchanged for the medium 4 h before imaging, and glucose was added at the indicated concentration to start the assay. During data acquisition (30 min) the myotubes were maintained at 37 °C on the microscope stage. Software developed for microscope image analysis (NIH Image) was used to compare brightness of the autofluorescence between cells.

Theoretical considerations

The rate expression for flux of a hexose tracer is:

$$ds_o/dt = \frac{([s_o]-[s_i])F_s}{1+[G_o]/K_{go}+[G_i]/K_{gi}+[G_i][G_o]/R_gB_g} \quad (1)$$

where K_{go}, K_{gi} and B_g are the Michaelis–Menton constants for glucose entry, exit and exchange, respectively, while s_o and s_i represent extracellular and intracellular tracer-labelled glucose or glucose analogues [14]. G_o and G_i are used for glucose concentrations in the denominator. Terms with picomolar concentrations of labelled glucose analogues divided by much larger Michaelis–Menton constants were not included. The coefficient F_s is the ratio V_{max}/K_m for the transporter and was specific for each analogue. R_g is dependent on the other constants:

$$R_g = \frac{1}{1/K_{go}+1/K_{gi}+1/B_g} \quad (2)$$

Cytochalasin B, which is considered a non-competitive inhibitor of glucose influx [15], reduces the clearance of glucose by a function that is essentially independent of glucose concentration, whereas a competitive inhibitor I_c (e.g. 3-*O*-methylglucose) has a diminished effect with increasing concentrations of unlabelled glucose. An approximate expression for the flux of a hexose tracer in the presence of inhibitors is:

$$-dS_o/dt = \frac{([S_o]-[S_i])F_s}{(D_t+I_c/K_c)(1+I_n/K_n)} \quad (3)$$

Here, S could be any hexose tracer, including D-[2-^{3}H]glucose. The symbol D_t represents the denominator of eqn (1). All the terms with glucose concentrations, including D_t, were recalculated as intracellular glucose changed as a function of time, medium concentration, inhibitor, etc. Both D_t and the denominator of eqn (4) (below) were unaffected by picomolar amounts of tracer hexoses divided by much larger affinity coefficients (K_m and K_i). I_c and I_n are the added concentrations of the competitive and non-competitive inhibitors, respectively. K_c and K_n are the respective inhibitory constants.

The equation for HK activity was simplified to the expression:

$$-dS_i/dt = \frac{F_{ps}[S_i]}{1+[G_i]/K_p} \quad (4)$$

Intracellular glucose (G_i) is treated as a simple competitive inhibitor for the phosphorylation of tracer, S. F_{ps} is the V_{max}/K_m ratio for HK, and is specific for glucose or its analogues.

The amount of intracellular hexose (including D-[2-^{3}H]glucose) at any time t is given by integration of the rates of glucose supply (eqn 3) minus glucose consumption (eqn 4). We can use $T_{01}[S_0-S_1]$ and $T_{02}[S_0-S_2]$ to represent eqn (3) for reversible transport between compartment 0 (medium) and two intracellular compartments. Likewise $P_{2,3}[S_2]$ will represent irreversible phosphorylation in compartment 2 to an outlet compartment, 3, while no phosphorylation occurs in compartment 1. We will postulate a factor, z, a fraction to proportion the cell volume between compartments 1 and 2. This makes it simpler to write and compute an integral with a phosphorylating compartment and a non-phosphorylating compartment in parallel, as follows:

$$S_1+S_2 = \int_0^t \{T_{02}([S_0]-[S_2])\cdot z + T_{01}([S_0]-[S_1])\cdot(1-z) - P_{23}[S_2]\cdot z\}\cdot dt \quad (5)$$

If z is equal to 1, the expression reduces to a single, phosphorylating compartment. But if z is less than one, a fraction of glucose is reversibly taken up by a compartment of volume $1-z$ (see below for a diagrammatic representation of this scheme). Eqn (5) was integrated, using the Runge–Kutta method with adaptive step-size control [16].

Statistics

The statistical significance of z, as well as individual coefficients of the model, were tested using Global Analysis (Globals Unlimited, Urbana, IL, U.S.A.) as described in the Results section. Otherwise, error distributions are expressed by S.E.M. or S.D. as noted, and statistical significance was determined by one-way ANOVA or by Student's paired t test.

RESULTS

Insulin stimulates glucose phosphorylation without a concomitant effect on measured transport or HK activities

The bulk glucose transport activity of the myotubes was estimated from the uptake of the non-metabolizable transport analogue of glucose, 3-*O*-methylglucose. The Michaelis–Menton coefficients for this transport measurement and the HK activity measured in cell lysates are given in Table 1. Whereas a 24 h treatment with 10 nM insulin increased transport by 20–30 % in some experiments, the effect of insulin on V_{max} and K_m of methylglucose transport was neither consistent nor significant in this cell line, although other sublines of L6 cells do show insulin-sensitive glucose transport [17]. The V_{max} of glucose phosphorylation in the extracts was not increased by insulin and was much greater

Table 1 Apparent values for glucose transport, phosphorylation and HK in L6 myotubes

Transport indicates the initial rates of 3-*O*-methylglucose transport. Phosphorylation was measured as ^3H_2O release from 2-[^{3}H]glucose to reflect coupled glucose transport and phosphorylation. HK is given as the HK activity in myotube extracts. *n* is the number of experiments performed.

	Insulin (10 nM)	K_m (mM)	V_{max} (nmol · h^{-1} · 100 μg^{-1})	*n*
Transport	−	5.7 ± 2.0	186 ± 36	6
Transport	+	6.1 ± 3.0	216 ± 30	6
Phosphorylation	−	1.1 ± 0.1	9.6 ± 2.4	6
Phosphorylation	+	1.1 ± 0.14	17.4 ± 1.2*	6
HK	−	0.1 ± 0.01	192 ± 12	2
HK	+	0.09 ± 0.01	186 ± 6	2

* Significantly different compared with control by non-paired Student's *t* test, $P < 0.01$.

than the V_{max} of glucose phosphorylation of the intact myotubes. The latter was doubled by the treatment with insulin. In addition, the K_m of HK in the extracts was lower than that of glucose phosphorylation in the intact myotubes.

Efflux and phosphorylation of glucose measured as parallel reactions

Phosphorylation and transport of intracellular glucose were measured transiently by an efflux assay (Figure 1). Before the assay, glucose utilization was allowed to proceed for 30 min with D-[2-^{3}H]glucose and 3-*O*-[^{14}C]methylglucose as tracers in the presence of 10 mM unlabelled glucose. The efflux assay showed less than a significant (20–40 %) increase in transport activity in insulin-treated cells (Figure 1, upper panel), while phosphorylation of glucose was elevated by an average of 1.8 ± 0.1-fold (Figure 1, lower panel). Data from three additional experiments were combined with the experiments represented in Figure 1 to show a significant stimulation by insulin ($P = 0.014$, $n = 6$). Glucose phosphorylation during the experiment occurred independently of transport since glucose already in the cells was no longer dependent on influx and the myotubes contained nearly equal concentrations of glucose when efflux was initiated. Only a small fraction of intracellular glucose was actually phosphorylated, while the rest was lost to efflux. The lines through the data in Figure 1 were generated by integration of eqn (5) for a two-compartment model as discussed below. Similar results were observed at a loading glucose concentration of 0.2 mM (results not shown). These results show that insulin increased the phosphorylation of glucose independently of any effects of the hormone on transport across the plasma membrane.

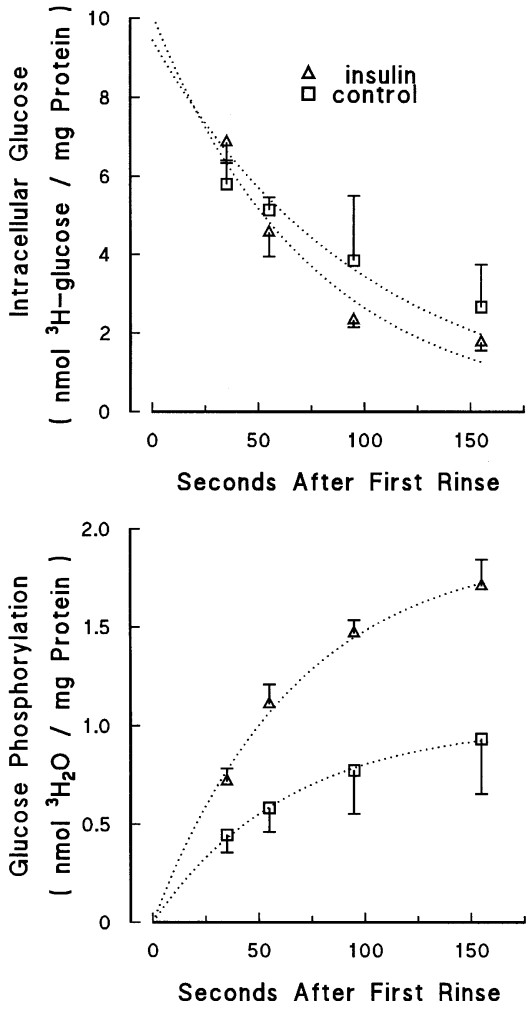

Figure 1 Efflux and phosphorylation of glucose measured in a parallel assay

Efflux was measured after 30 min preincubation of 1 cm wells of L6 myotubes with medium (HBS) containing 10 mM D-[2-^{3}H]glucose. Where indicated, the cells were treated 24 h prior to this and during pre-incubation with 10 nM insulin. Intracellular glucose (upper panel) remaining in the myotubes was estimated by calculating back from the amounts of ^3H_2O released (lower panel), and glucose that effluxed into the medium (results not shown). The means ± S.E.M. from three separate experiments are shown for control (□) and insulin-stimulated (△) myotubes. The lines through the data were generated by integration of eqn (5) for a two-compartment model as discussed in the text.

Intracellular hexose concentrations

Myotubes attained steady-state concentrations of 3-*O*-[^{14}C]-methylglucose and D-[2-^{3}H]glucose within minutes (Figure 2). The space for L-[^{3}H]glucose measured after washing to remove most extracellular sugar remained at 0.14 μl/mg throughout the experiment. The calculation of intracellular hexose amounts to a minimum estimate, since some of the D-[2-^{3}H]glucose would have been detritiated and lost, while 2-deoxy-[1-^{14}C]glucose would have been phosphorylated to some extent and lost during the anion-exchange step. Nonetheless glucose and 3-*O*-methylglucose appeared to distribute nearly equally in approx. 1 μl of space/mg of cell protein at steady state, within the error range of the measurement. This suggested that transport of hexoses into the bulk cytoplasm greatly exceeded the activity of phosphorylation to deplete them.

Influence of transport inhibitors on intracellular hexose concentrations

Selective inhibition of transport should allow phosphorylation to deplete intracellular glucose maximally relative to 3-*O*-methylglucose, which is not a HK substrate. Up to 50 mM 3-*O*-methylglucose (Figure 3, left-hand panel) and up to 1 μM cytochalasin B (Figure 3, right-hand panel) failed to prevent the accumulation of intracellular glucose tracer below half of what it was in the absence of inhibitors. Similar results were observed

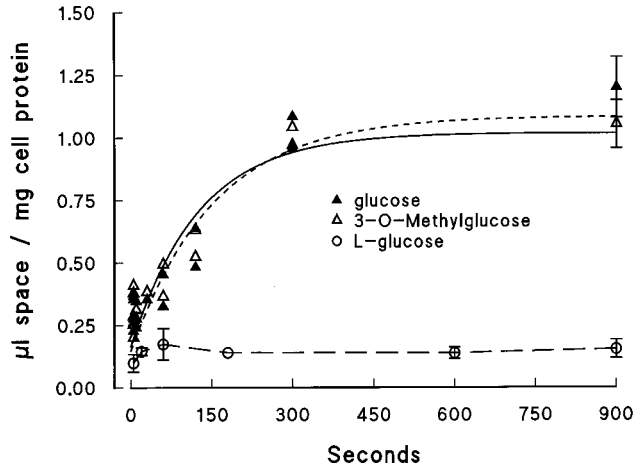

Figure 2 Time course of hexose tracer entry

All wells were preincubated for 30 min with HBS containing insulin and 5 mM glucose at room temperature. This was replaced with HBS containing 5 mM glucose, D-[2-^{3}H]glucose (▲, short-dashed line) and 3-*O*-[^{14}C]methylglucose (△, solid line) and, in separate wells, L-[^{3}H]glucose (○, long-dashed line). At the indicated times, the wells were rinsed and extracted to measure unphosphorylated hexoses as described in the Experimental section. Spaces for each hexose are shown without a correction for extracellular space. Symbols with bars represent means ± S.E.M. from 3–8 determinations.

when 2-deoxyglucose was compared with 3-*O*-methylglucose (results not shown). The data were modelled using eqn (5), and lines are drawn to show the expected results with fitting to either a one- or two-compartment model. It is clear that these data were poorly fitted by the one-compartment model. In a two-compartment model, only about 15% of the cell could potentially be depleted of glucose by phosphorylation in the presence of a combination of low (0.2 mM) glucose and high concentrations of transport inhibitors in the medium.

The postulate of a small compartment for glucose uptake in L6 myotubes was supported by other data. Phosphorylation of D-[2-^{3}H]glucose was sensitive to 3-*O*-methylglucose acting as a competitive inhibitor of glucose transport (Figure 4, left-hand panels), and was even more sensitive to cytochalasin B (Figure 4, right-hand panels). The apparent K_i for cytochalasin B inhibition at 0.2 mM glucose was 0.1 μM, while at 5 mM glucose the K_i was 0.5 μM. The simplest explanation for this behaviour is that intracellular glucose in a critical compartment is sensitive to inhibition of glucose transport. Figure 3 shows a slight effect of the inhibitors leading to reduced accumulation of intracellular glucose that is consistent with this hypothesis.

Relative clearances of D-[2-^{3}H]glucose and 2-deoxy-[1-^{14}C]glucose discriminate between insulin's effect on glucose transporters and HKs

Control of glucose phosphorylation as a pathway was further defined by the ratio of clearances of different hexose tracers. The ratio of the clearances of glucose and 2-deoxyglucose tracers by the different HKs shows a 5–10-fold preference for glucose [18]. The transporters show little preference (1:1 ratio of clearances) when initial rate of uptake (transport rate) is measured [4]. At 0.2 mM glucose (Figure 5, upper panel) the ratio of clearance of 2-deoxyglucose to glucose tracer was close to unity, indicating that transport was rate-limiting. At 5 mM glucose in insulin-treated myotubes, HK was rate-limiting, since the ratio of the clearances of deoxyglucose to glucose tracers was 0.3–0.4 (Figure 5, lower panel). When cytochalasin B was added with 5 mM glucose to inhibit transport relative to HK, the ratio of clearances was restored to the former value, consistent with inhibition of transport to a rate-limiting condition.

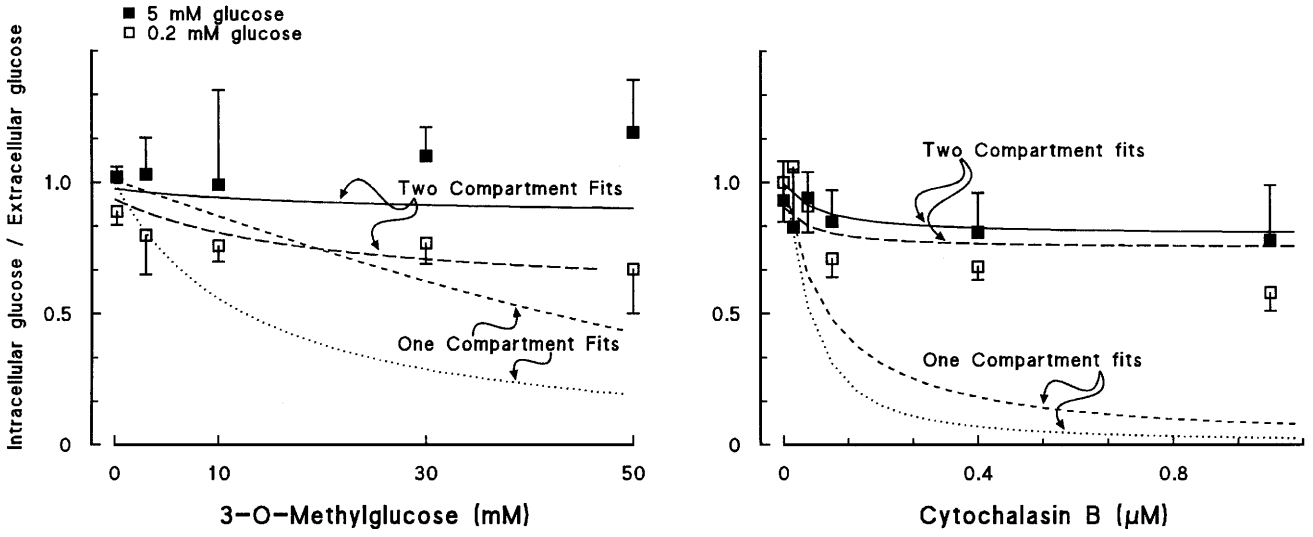

Figure 3 Intracellular hexose spaces

Myotubes were incubated with HBS and 0.2 mM (□) or 5 mM (■) unlabelled glucose, plus tracer amounts of D-[2-^{3}H]glucose and 3-*O*-[^{14}C]methylglucose. In the left-hand panel, incubations contained the indicated concentrations of unlabelled 3-*O*-methylglucose, and in the right-hand panel cytochalasin B was added at the concentrations noted. After 60 min of incubation at 37 °C, the myotubes were rinsed and extracted (see the Experimental section). The space for D-[2-^{3}H]glucose is shown as intracellular glucose, while the space for 3-*O*-[^{14}C] methylglucose was used to represent the space glucose would occupy if the ratio of intracellular/extracellular glucose was unity. Means ± S.E.M. from triplicate incubations are shown with lines indicating fits of the data to either a one- (dotted line, 0.2 mM glucose; short-dashed line, 5 mM glucose) or two- (long-dashed line, 0.2 mM glucose; solid line, 5 mM glucose) compartment model.

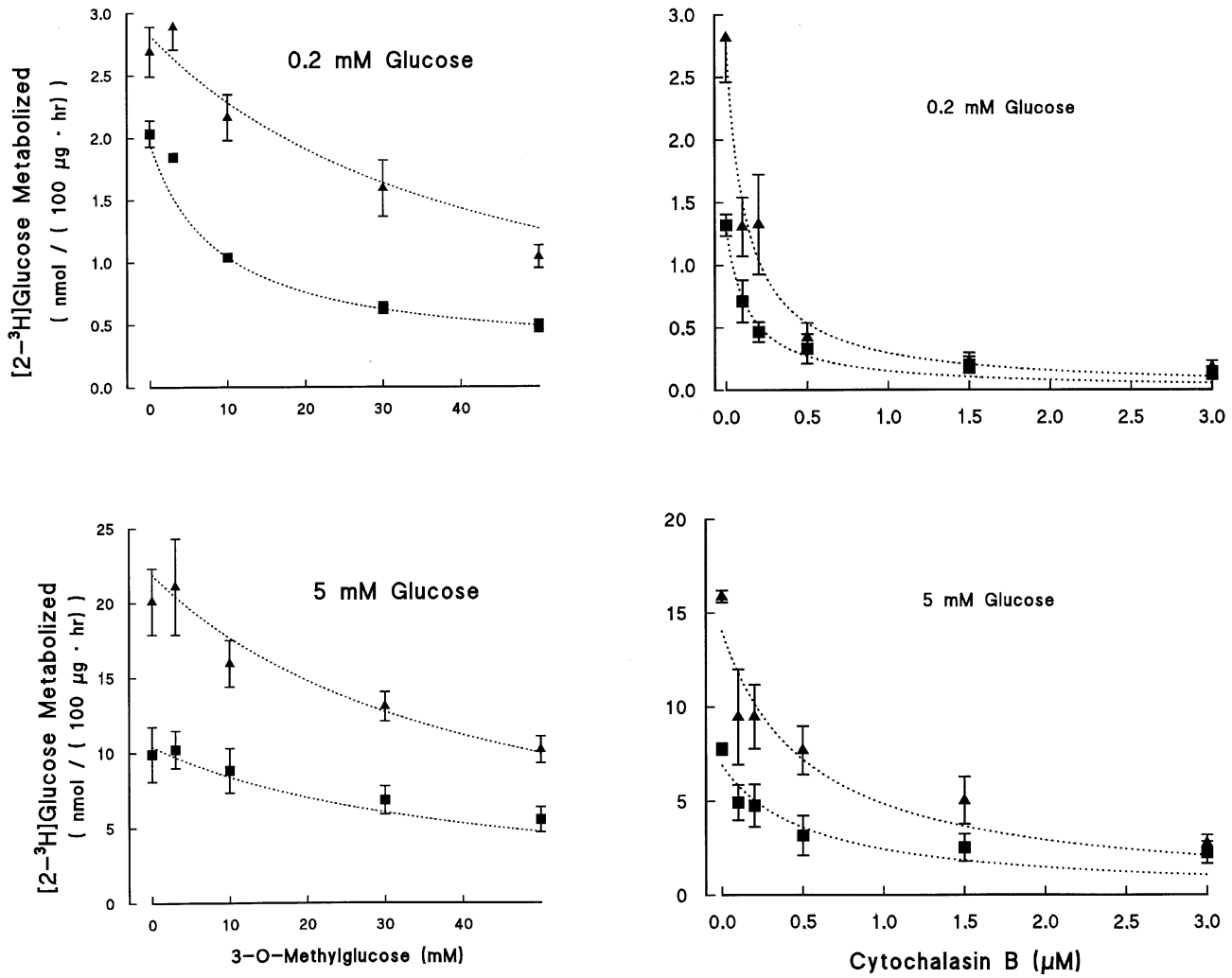

Figure 4 Effects of transport inhibitors on L6 myotube glucose phosphorylation

Control (■) and insulin-treated (▲) myotubes were incubated at 37 °C for 30 min in HBS containing D-[2-^{3}H]glucose, 2-deoxy-[1-^{14}C]glucose and either 0.2 mM (upper panels) or 5 mM (lower panels) unlabelled glucose. 3-*O*-Methylglucose (left-hand panels) or cytochalasin B (right-hand panels) were present at the indicated concentrations. Phosphorylation was measured as described in the Experimental section. Lines through the data are fits to a two-compartment model for transport and phosphorylation of glucose. Means ± S.E.M. from 3–5 experiments are shown.

Intracellular G6P

G6P, a product and feedback inhibitor of HK, is likely to be the major intracellular limit on phosphorylation of glucose when present at significant concentrations. It was elevated in the presence of insulin and glucose in the medium (Figure 6). This suggested that the locus of insulin's major effect on the rate of glucose utilization was on glucose transport and/or glucose phosphorylation. Insulin stimulation primarily of enzymes downstream of HK would have increased the flux of G6P and decreased its concentration in the cell.

Error estimates for the insulin stimulation of glucose phosphorylation

Analysing the data globally (see the Experimental section) provided an estimate of confidence for each parameter of the model by testing the impact of changes in its value upon the global χ^2 (the measure of the goodness of fit to the entire set of data). HK V_{max} was found to be the most critical factor after the factor z (discussed below). The analysis was used to test the significance of the effect of insulin to increase the HK V_{max} (apparent) in intact myotubes (Figure 7). The increase in HK V_{max} (actual) was greater than indicated by phosphorylation activity alone when the inhibition by elevated G6P is considered. However, G6P was not included in the model since its effect depends on other factors that were not measured (HK isoforms, HK binding to mitochondria, concentrations of ATP and other HK ligands). The dotted line corresponds to two S.D.s from the mean, or a confidence level of 0.67. The intersection of the two curves marks the deviation that would result if the V_{max} in the presence of insulin were the same as the control. Since the intersection is above the dotted line, we concluded the difference in the two V_{max} values to be significant. Ranges of global χ^2 values were calculated for other parameters and given in Table 2. This treatment of the data also shows that the K_m of glucose phosphorylation was unaltered by insulin. Combining the data from deoxyglucose measurements with glucose measurements and analysing the data globally strengthened the reliability of both the HK and the transporter determinations. The analysis included the experiments shown in Figures 1–5.

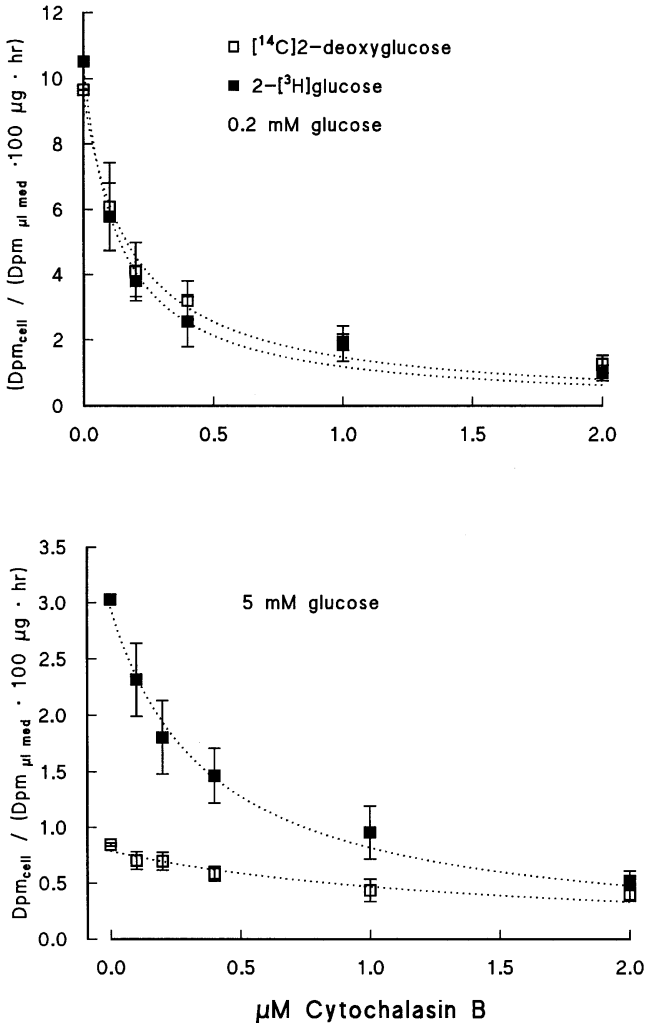

Figure 5 Clearance of glucose and 2-deoxyglucose tracers

Each of the glucose-phosphorylation experiments depicted in Figure 4 included 2-deoxy-[1-^{14}C]glucose (□) as well as D-[2-^{3}H]glucose (■) as tracers. The upper panel shows the effects of increasing concentrations of cytochalasin B on uptake of both tracers in insulin-stimulated myotubes at 0.2 mM glucose, while the bottom panel shows the clearance at 5 mM glucose. The lines through the data are fits to a two-compartment model.

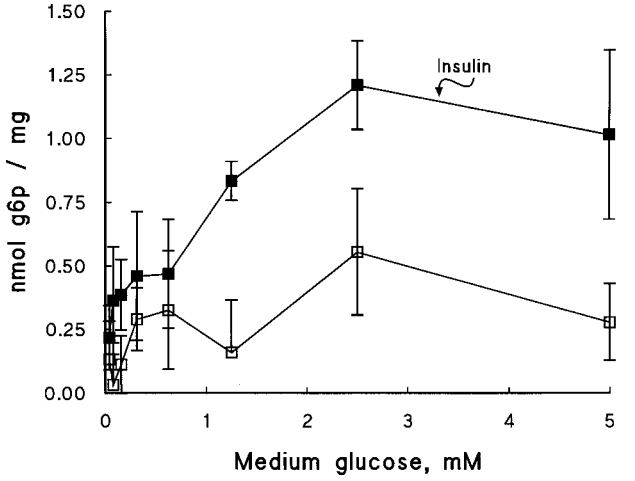

Figure 6 Effect of insulin and glucose on intracellular G6P concentrations

G6P was measured following an overnight incubation of myotubes with 5 mM glucose and 10 nM insulin as noted. The cells were rinsed three times with DMEM without glucose. Then DMEM with the glucose concentrations shown and insulin as noted were added and the cells were incubated 30 min at 37 °C in 5% CO_2. Extracts were prepared and the G6P content was measured as described in the Experimental section. In this figure, 1 nmol of G6P/mg of cell protein represents a 1 mM concentration in the cell, since 1 mg of cell protein represents approx. 1 μl of intracellular water. The points shown are means from a representative experiment with error bars (S.D.) corresponding to 4–6 determinations.

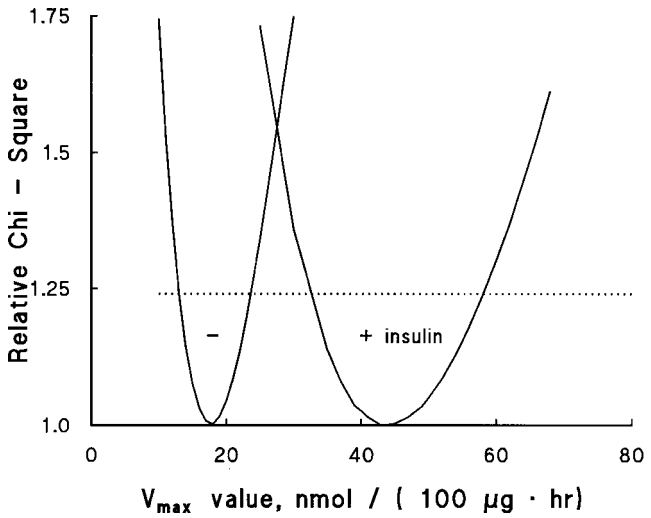

Figure 7 Analysis of glucose phosphorylation from intact cell data

The entire data set in Figures 4 and 5 was fit globally using varied V_{max} values for phosphorylation (HK) for control and insulin-treated myotubes while the other parameters were allowed to float in compensation. A χ^2 value was obtained at each value and divided by the minimum χ^2. The dotted horizontal line was drawn at the χ^2 value corresponding to the S.E.M. of the data set.

The coefficient z (Table 2) was intended to represent the fraction of the cytoplasm having insulin-sensitive glucose transporters and the ability to phosphorylate glucose. However, cellular heterogeneity would account for this behaviour if the cells included some that were metabolically inert during the assays. To test for this we used two-photon excitation microscopy (see the Experimental section) to monitor glucose-dependent NAD(P)H autofluorescence. Two-photon laser imaging microscopy measures the autofluorescence of NAD(P)H in individual cells reflecting primarily the ratio NADH/NAD in mitochondria [19]. This measurement has been shown to be sensitive to increases in glucose phosphorylation in a variety of cells [13]. We used this technique to show that the great majority of L6 myotubes in culture are metabolically active and respond uniformly to increases in concentration of glucose (results not shown). This ruled out the possibility that metabolically inactive myotubes could account for our results.

Analysis of compartmentalization of glucose uptake

The calculated transport parameters of Table 2 are in sharp disagreement with the measured transport parameters in Table 1. The latter were derived from the experiments shown in Figures 1–3. The data of Figures 4 and 5, when analysed globally, were the source of the parameters in Table 2. The data shown in Figure 3 are better fitted using a combination of the two sets of

Table 2 Model parameters for transport/phosphorylation

The units of V_{max} are nmol · h^{-1} · 100 μg^{-1}. Global parameters represent other coefficients from eqns (1)–(5). These were not evaluated separately with and without insulin.

Parameter	− Insulin	+ Insulin
Transport		
K_{go} (= R_g)	2.6 ± 0.8 mM	1.3 ± 0.4 mM
V_{max} (F_s/K_{go})	70 ± 14	100 ± 20
HK		
K_p	0.09 ± 0.02 mM	0.09 ± 0.01 mM
V_{max} (F_p/K_p)	18 ± 6*	44 ± 9*
Global parameter		
z	0.15 ± 0.04	
$F_{s(deoxyglucose)}/F_{s(glucose)}$	0.89	
$F_{p(deoxyglucose)}/F_{p(glucose)}$	0.07	
$K_{i(cytochalasin\ B)}$	0.067 μM	
$K_{c(methylglucose)}$	32 mM	
K_{gi} (= B_g)	300 mM	

* Significantly different by error analysis.

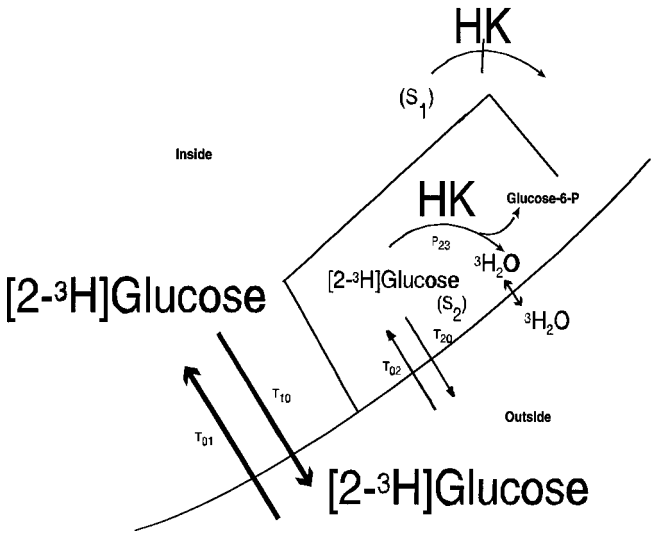

Figure 8 Schematic diagram of the two-compartment model for glucose transport and phosphorylation

The model illustrates how a system of equations could reconcile the various types of experiments with a small compartment for phosphorylation. The smaller of two intracellular compartments (z in eqn 5) is separated schematically from the bulk of the cell, $1-z$, while relative hexose concentrations ([S_1] and [S_2] in eqn 5) are indicated by the font size given to [2-^{3}H]glucose. Glucose is close to the medium concentration ([S_0] in eqn 5) in the bulk of the cell (compartment $1-z$), and it is lower in the smaller compartment ([S_2] and z in eqn 5). Compartment $1-z$ contains only inactive or inhibited HK represented by a crossed arrow, while compartment z contains the active HK. The arrows are labelled T for transport and P for phosphorylation, with the subscripts that define the direction of movement from one compartment to the next as discussed in the text.

parameters in a two-compartment model. The solid lines in Figure 3 are drawn according to the two-compartment model, with the dashed lines drawn to illustrate the comparison of this model with a one-compartment model. Figure 8 depicts the two-compartment model outlined in the Experimental section. This model includes a parameter, z, to represent the volume of the cell participating in phosphorylation of glucose, while the fraction $1-z$ occupies the rest of the cell and is metabolically inert with regard to glucose phosphorylation. All the data can be accounted for by a value for z comprising 15% of the volume. The ranges for S.D. given for the values of Table 2 are from the global confidence limits established as described for HK above. Two-fold symmetry of the transport reaction was assumed: $K_g = R_g$. K_{gi} was set equal to B_g and arbitrarily given the value of 300 mM in line with the very low affinity of the inside-facing glucose carrier of other cell types [20]. The parameter deoxyglucose/glucose was the ratio of the activities for hexose tracers as substrates. The prediction that this ratio was 0.89 for the transport reaction was consistent with measurement of initial rates of uptake in intact cells, and the predicted ratio of 0.07 was consistent with measured phosphorylation in cell lysates. These values were fixed during the confidence determination of the other parameters that could not be measured independently.

DISCUSSION

L6 myotubes have been used extensively as a cellular model to help understand glucose uptake in muscle independently of the special geometry and control of blood flow that occur *in vivo*. The subline used here had high glucose transport activity compared with others [15]. This seemed to make these cells a particularly good model to look at possible effects of insulin on HK by measuring phosphorylation-limited glucose uptake. Phosphorylation by HK is the first committed step in glucose utilization and is a logical control point for subsequent steps. Overnight insulin treatment of L6 myotubes increases glucose utilization, HK II mRNA and synthesis of new HK II protein by 2–3-fold [7]. The newly synthesized HKII does not appear to add significantly to total HK, but it might bind mitochondria preferentially, where it is known to phosphorylate glucose with greater efficiency [21].

Metabolic control analysis in several cell types has revealed that activity of HK (and other enzymes) seen in cell extracts is not a reliable indicator of activity available in the cell [22]. We sought to define insulin's control over glucose phosphorylation using intact cells. One experiment assessed the action of insulin on glucose transport and phosphorylation measured transiently (Figure 1). Other experiments were designed to measure the coupled reactions of transport and phosphorylation at the steady state.

Glucose transport did not appear to limit phosphorylation or account for the ability of insulin to regulate it when both reactions were measured directly (Figure 1). Steady-state measurements suggested, however, that transport shared control of glucose phosphorylation. Both 3-*O*-methylglucose and cytochalasin B decreased glucose phosphorylation as if intracellular glucose were low. Further, the apparent K_m of glucose phosphorylation was about 1 mM, a value higher than that of phosphorylation of glucose in lysates (0.1 mM), implying that the glucose concentration where HK was located was less than that in the medium at any given extracellular glucose concentration.

In general, experiments that directly measured glucose transport yielded parameters that were significantly different from parameters that were extrapolated from an array of steady-state metabolic data. Two possibilities could account for these discrepancies: (1) a subset of transporters is insulin-sensitive and associated only with a small compartment, with insulin-insensitive transporters serving the bulk of the cytoplasm, or (2) an artifact with most myotubes dead or dying without the ability to phosphorylate glucose though able to transport and accumu-

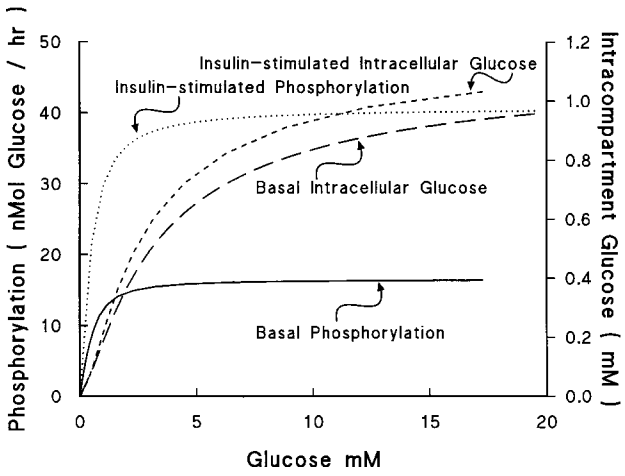

Figure 9 Model predictions of compartmental glucose concentrations

Values from Table 2 were used to simulate glucose phosphorylation and glucose in the phosphorylating compartment of the hypothesized model. The phosphorylation curve corresponds to measurement, while intracompartment glucose is a prediction.

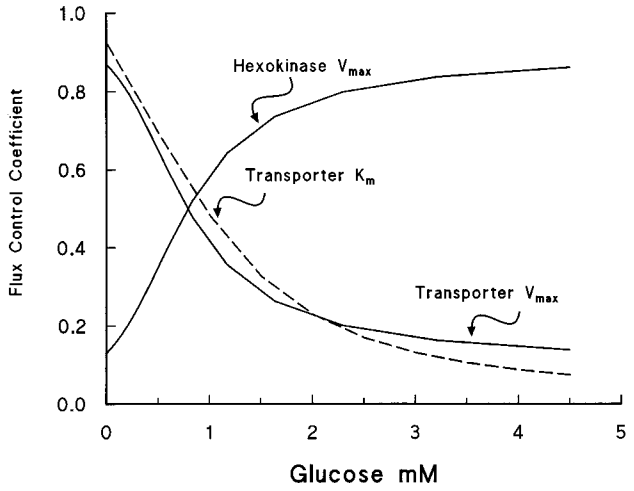

Figure 10 FCCs

FCCs were calculated for the parameters of transporter K_m, transporter V_{max} and HK V_{max} for a range of medium glucose concentrations. The calculation was made from the fractional change in phosphorylation rate attributable to a minute change in the parameter values of Table 2.

late it. The latter possibility was ruled out by the observation of nearly uniform NAD(P)H autofluorescence among the cells.

Substrate specificity was also used to study how glucose uptake is limited. The clearance ratio, deoxyglucose/glucose, was used to relate substrate specificity to limits on glucose utilization under various conditions including cytochalasin B. When analysed globally, clearance ratios and the various other data provided robust estimates of the factors that limit glucose uptake. Global Analysis, a computer program designed to fit and perform error analysis on complex, multidimensional fluorescence lifetime spectra [8], proved to be a valuable tool for our studies. The program was modified to perform multidimensional analysis of different experiments according to common parameters for glucose transport and phosphorylation. Using this program, we demonstrated that two intracellular compartments fit the obtained data better than one intracellular compartment.

The existence of a compartment to explain the contradicting results obtained in other systems has been suggested [9]. A two-compartment model predicts intracellular glucose levels close to the K_m of HK in the hypothetical phosphorylating compartment and predicts that these levels remain relatively constant when phosphorylation is doubled by insulin, due to a balanced increase in the rate of glucose transport and phosphorylation (Figure 9).

Transporters and HKs together catalyse the phosphorylation reaction that generates G6P, which rose significantly with increased glucose concentrations and stimulation by insulin. Increased flux through the pathway downstream of HK could be explained by increased G6P controlled through the combined reactions of transport and phosphorylation of glucose. The individual control strengths of transport and HK may be further defined by flux-control coefficients (FCCs) [22]. Figure 10 shows the FCC for the parameters that were affected in the present studies: transporter V_{max}, transporter K_m and HK V_{max}. A change in the overall rate of transport/phosphorylation is affected by a very small change (0.1 %) in either transporter K_m or V_{max} by almost a one-to-one equivalence when the medium glucose is low (FCC near 1 at 0.2 mM glucose). At 5 mM glucose the overall rate still changes in response to a change in transporter V_{max}, but now by a considerably lower 0.1-to-1 equivalence (FCC $\approx$ 0.1). At 5 mM glucose the FCC of a change in transporter K_m is even less. Thus, the two-compartment model accounts well for the observation that small amounts of cytochalasin B were able to inhibit phosphorylation at 5 mM medium glucose, while smaller amounts inhibit phosphorylation at 0.2 mM medium glucose. The figure also illustrates how insulin might stimulate glucose phosphorylation at 0.2 mM glucose mostly by stimulating transporter (K_m or V_{max}) and at 5 mM glucose mostly by stimulating HK. If transport alone was stimulated, a much-reduced effect of insulin would be seen at 5 mM glucose, while in fact the effect of insulin is somewhat higher at higher glucose concentrations. These observations suggest that the effect of an overnight treatment with insulin has a somewhat greater effect on HK than on transport, an effect that is even greater when G6P inhibition is taken into account.

Possible bases for compartmentalization include the participation of certain transporters and HKs in substrate channelling [23], or sequestration of active HK bound to mitochondria [24]. Previous observations that insulin increases the fraction of HK bound to the mitochondria [21], where the enzyme may be more active [25] and less sensitive to inhibition by G6P [26] support the latter possibility. A compartmentalization of HK into G6P-sensitive and -insensitive pools might accompany the sequestration of insulin-sensitive glucose transporters, and this has been suggested as a mode of insulin action [27]. The physiological basis of the two-compartment model adopted in the present studies is unknown. The existence of barriers to intracellular diffusion of hexoses has been suggested [28]. Such barriers would separate glucose in a small compartment containing active HK from the remainder of the glucose and inactive HK in the cytoplasmic space (Figure 8).

In conclusion, the extent to which our findings in L6 myotubes apply to intact skeletal muscle is difficult to assess. For example, L6 myotubes differ from skeletal muscle myocytes in that they have substantial amounts of the glucose transporter GLUT1 [29]. This probably accounts for the high capacity for glucose transport observed in these cells. However, the excess glucose uptake into the bulk cytoplasm allowed us to detect the presence of a distinct compartment served by insulin-sensitive glucose

transporters, possibly GLUT4. Such a space may be broadly important to interpret the hormonal response of glucose transport where GLUT4 and GLUT1 are present together. This situation exists also in skeletal muscle, where the distribution of the control of glucose metabolism between glucose transporters and HK is still controversial.

This work was jointly funded by the Department of Veterans Affairs and the Juvenile Diabetes Foundation International, and by National Institutes of Health (NIH) grants DK46867-06 (to D. K. G.), DK20593 (to D. K. G.), DK53434 (to D. W. P.) and NSFBRI-9871063 (to D. W. P.). Two-photon experiments were performed in part through the use of the Vanderbilt University School of Medicine Cell Imaging Core Resource (supported by NIH grants CA68485 and DK20593).

REFERENCES

1 Rothman, D. L., Magnusson, I., Cline, G., Gerard, D., Kahn, C. R., Shulman, R. G. and Shulman, G. I. (1995) Decreased muscle glucose transport/phosphorylation is an early defect in the pathogenesis of non-insulin-dependent diabetes mellitus. Proc. Natl. Acad. Sci. U.S.A. **92**, 983–987

2 Bonadonna, R. C., Del Prato, S., Bonora, E., Saccomani, M. P., Gulli, G., Natali, A., Frascerra, S., Pecori, N., Ferrannini, E., Bier, D. M. et al. (1996) Roles of glucose transport and phosphorylation in muscle insulin resistance of NIDDM. Diabetes **45**, 915–925

3 Whitesell, R. R., Aboumrad, M. K., Powers, A. C., Regen, D. M., Le, C., Beechem, J. M., May, J. M. and Abumrad, N. A. (1993) Coupling of glucose transport and phosphorylation in *Xenopus* oocytes and cultured cells: determination of the rate-limiting step. J. Cell. Physiol. **157**, 509–518

4 LeFevre, P. G. (1961) Sugar transport in the red blood cell: structure-activity relationships in substrates and antagonists. Pharmacol. Rev. **13**, 39–70

5 Jacobs, A. E. M., Oosterhof, A. and Veerkamp, J. H. (1990) 2-Deoxy-D-glucose uptake in cultured human muscle cells. Biochim. Biophys. Acta **1051**, 230–236

6 Ashcroft, S. J. and Stubbs, M. (1987) The glucose sensor in HIT cells is the glucose transporter. FEBS Lett. **219**, 311–315

7 Osawa, H., Printz, R. L., Whitesell, R. R. and Granner, D. K. (1995) Regulation of hexokinase II gene transcription and glucose phosphorylation by catecholamines, cyclic AMP, and insulin. Diabetes **44**, 1426–1432

8 Beechem, J. M. (1992) Global analysis of biochemical and biophysical data. Methods Enzymol. **210**, 37–54

9 Halseth, A. E., Bracy, D. P. and Wasserman, D. H. (2001) Functional limitations to glucose uptake in muscles comprised of different fiber types. Am. J. Physiol. Endocrinol. Metabolism **280**, E994–E999

10 Katz, J. and Dunn, A. (1967) Glucose-2-*t* as a tracer for glucose metabolism. Biochemistry **6**, 1–5

11 Gots, R. E. and Bessman, S. P. (1973) An ultrasensitive radioassay for hexokinase. Anal. Biochem. **52**, 272–279

12 Ardehali, H., Yano, Y., Printz, R. L., Koch, S., Whitesell, R. R., May, J. M. and Granner, D. K. (1996) Functional organization of mammalian hexokinase II. Retention of catalytic and regulatory functions in both the NH_2- and COOH-terminal halves. J. Biol. Chem. **271**, 1849–1852

13 Bennett, B. D., Jetton, T. L., Ying, G., Magnuson, M. A. and Piston, D. W. (1996) Quantitative subcellular imaging of glucose metabolism within intact pancreatic islets. J. Biol. Chem. **271**, 3647–3651

14 Regen, D. M. and Tarpley, H. L. (1974) Anomalous transport kinetics and the glucose carrier hypothesis. Biochim. Biophys. Acta **339**, 218–233

15 Klip, A. (1982) Regulation of glucose transport by insulin and non-hormonal factors. Life Sci. **31**, 2537–2548

16 Press, W. H. (1988) Numerical Recipes in FORTRAN, the Art of Scientific Computing, Cambridge University Press, Cambridge

17 Klip, A., Guma, A., Ramlal, T., Bilan, P. J., Lam, L. and Leiter, L. A. (1992) Stimulation of hexose transport by metformin in L6 muscle cells in culture. Endocrinology **130**, 2535–2544

18 Grossbard, L. and Schimke, R. T. (1966) Multiple hexokinases of rat tissues. Purification and comparison of soluble forms. J. Biol. Chem. **241**, 3546–3560

19 Williams, R. M., Piston, D. W. and Webb, W. W. (1994) Two-photon molecular excitation provides intrinsic 3-dimensional resolution for laser-based microscopy and microphotochemistry. FASEB J. **8**, 804–813

20 Whitesell, R. R. and Regen, D. M. (1978) Glucose transport characteristics of quiescent thymocytes. J. Biol. Chem. **253**, 7289–7294

21 Bessman, S. P. (1966) A molecular basis for the mechanism of insulin action. Am. J. Med. **40**, 740–749

22 Fell, D. A. and Sauro, H. M. (1990) Metabolic control analysis by computer: progress and prospects. Biomed. Biochim. Acta **49**, 811–816

23 Minaschek, G., Gröschel-Stewart, U., Blum, S. and Bereiter-Hahn, J. (1992) Microcompartmentation of glycolytic enzymes in cultured cells. Eur. J. Cell Biol. **58**, 418–428

24 Rose, I. A. and Warms, J. V. B. (1967) Mitochondrial hexokinase. Release, rebinding and location. J. Biol. Chem. **242**, 1635–1645

25 Kosow, D. P. and Rose, I. A. (1968) Ascites tumor mitochondrial hexokinase II. Effect of binding on kinetic properties. J. Biol. Chem. **243**, 3623–3630

26 de Cerqueira, C. M. and Wilson, J. E. (2001) Functional characteristics of hexokinase bound to the type A and type B sites of bovine brain mitochondria. Arch. Biochem. Biophys. **397**, 106–112

27 Bessman, S. P. and Geiger, P. J. (1980) Compartmentation of hexokinase and creatine phosphokinase, cellular regulation, and insulin action. Curr. Topics Cell. Regul. **16**, 55–86

28 Bunow, B. (1978) Chemical reactions and membranes: a macroscopic basis for facilitated transport, chemiosmosis, and active transport. Part 1: linear analysis. J. Theor. Biol. **75**, 51–78

29 Estrada, D. E., Ewart, H. S., Tsakiridis, T., Volchuk, A., Ramlal, T., Tritschler, H. and Klip, A. (1996) Stimulation of glucose uptake by the natural coenzyme α-lipoic acid/thioctic acid: participation of elements of the insulin signaling pathway. Diabetes **45**, 1798–1804

Received 9 August 2002/24 October 2002; accepted 31 October 2002
Published as BJ Immediate Publication 31 October 2002, DOI 10.1042/BJ20021256